AIP Journal of Applied Physics

Quantitative analysis of fiber texture in cubic films

Satish Rao and C. R. Houska

Citation: Journal of Applied Physics **54**, 1872 (1983); doi: 10.1063/1.332240
View online: http://dx.doi.org/10.1063/1.332240
View Table of Contents: http://scitation.aip.org/content/aip/journal/jap/54/4?ver=pdfcov
Published by the AIP Publishing

Quantitative analysis of fiber texture in cubic films

Satish Rao and C. R. Houska
Department of Materials Engineering, Virginia Polytechnic Institute and State University, Blacksburg, Virginia 24061

(Received 7 September 1982; accepted for publication 11 November 1982)

The method of Roe and Krigbaum for determining fiber texture has been extended to thin film applications. It is often desirable to make *in situ* pole density measurements of a film on a thick substrate. This does not permit complete data to be collected by x-ray transmission techniques. If the data are restricted to the range $0 \leqslant \chi \leqslant 75°$, obtained by reflection, incomplete pole density plots are obtained, and it is necessary to devise a self-consistent extrapolation technique that extends the pole density data to 90°. This requires least-squares fitting over the range from $\chi = 0$ to 75° and an iterative procedure for extrapolating with functions consistent with a single orientation function. The example of a 1.14-μ Mo film on a (111) Si substrate requires an expansion of the symmetry relations to order 46. The procedure established herein is readily extended to include the effect of static displacements resulting from embedded gas atoms that are associated with sputtered films.

PACS numbers: 68.60. + q

INTRODUCTION

Roe and Krigbaum[1] presented a technique for analyzing x-ray diffraction data from polycrystalline samples having a fiber texture. In this paper, their quantitative analysis is extended to films with a cubic crystal structure and thick substrates. Only incomplete pole figure data can be obtained because of the inability to use x-ray transmission techniques and still keep the film intact. Morris[2] has given a least-squares technique for determining the orientation function from incomplete pole figures. The method is complicated by the loss of orthogonality relations among the associated Legendre functions used in the analysis.

Rao and Houska[3] have suggested a technique to extrapolate each pole figure data separately. It was found that the extrapolations obtained from such a procedure need not always be mutually consistent. Here, it is shown that the unmeasured region of the plane normal distributions may at first be approximated with a straight line, such that the area under the curve of the plane normal distributions is normalized and the functions remain orthogonal. By using an iterative technique, the plane normal distributions are continuously refined in the unmeasured region until a predetermined accuracy is achieved. Also, the thickness of the film is estimated by performing successive iterations with different thickness values until a thickness is found that satisfies the normalization requirement within the experimental range of uncertainty.

X-ray diffraction data of six plane normal distributions were obtained from a Mo film sputtered onto a (111) Si single crystal substrate. The data could be obtained only to 75° in $\chi_{hk\ell}$ (angle between the normal to the $(hk\ell)$ crystallographic plane and the fiber axis). This method is used to obtain the orientation function for the polycrystalline film from limited x-ray diffraction data. To determine the effect of χ truncation, the procedure is repeated with $\chi_{\max} = 60°$ and 45°, for all the plane normal distributions. The discrepancies found with respect to $\chi_{\max} = 75°$ are well within experimental error even when using data restricted to 45°. If the same analysis is performed using the data for only five plane normal distributions, deviations can be observed with the sixth although the general nature of the curves remain the same. Legendre polynomials till order 46 are required to fit the Mo plane normal distribution curves satisfactorily. It is also found that the method of initial extrapolation to the plane normal distribution curves in the unmeasured region does not significantly affect the results.

DEFINITION OF EULER ANGLES

The orientation of a rigid body in space can be completely specified using the Euler angles Ω, Ψ, and ϕ or the equivalent ϵ, ψ, and ϕ, where $\epsilon = \cos \Omega$. These angles are illustrated in Fig. 1. Let 0-xyz be a system of mutually orthogonal

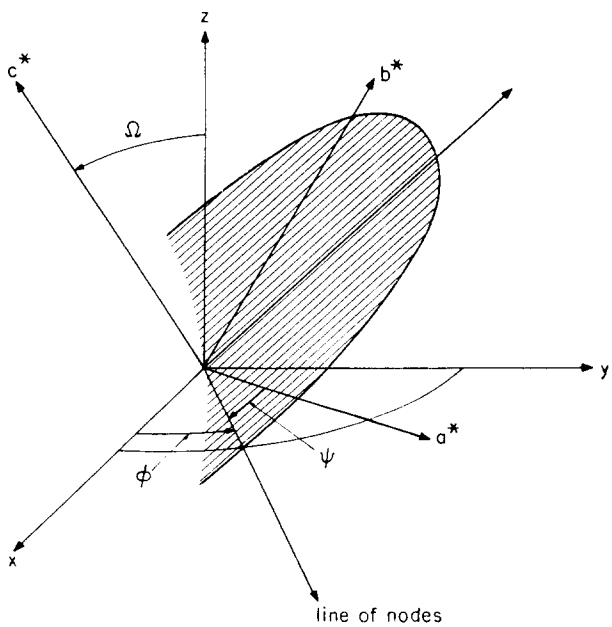

FIG. 1. Illustration of Euler angles Ω, ϕ, and ψ as they relate to the reciprocal lattice of one crystallite.

 0021-8979/83/041872-11$02.40

axes fixed in the polycrystalline sample with the z axis coinciding with the fiber axis. The axes 0-$a^*b^*c^*$ are a second orthogonal system fixed in the crystallite. For convenience, a^*,b^*,c^* are the reciprocal axes for the crystal axes a, b, and c. The plane perpendicular to the axis c^* intersects the xy plane along the line of nodes. The angle ϕ is confined to the xy plane, between the x axis and the line of nodes. The angle ψ is measured in the plane perpendicular to axis c^*, and is the angle between the a^* axis and the line of nodes. The angle Ω is the angle between the z and c^* axis. The matrix of the complete transformation from the xyz coordinate system to the $a^*b^*c^*$ coordinate system can be shown to be equal to

$$T(\phi,\Omega,\psi)=\begin{bmatrix} \cos\psi\cos\Omega\cos\phi-\sin\psi\sin\phi & \sin\phi\cos\Omega\cos\psi+\cos\phi\sin\psi & -\sin\Omega\cos\psi \\ -\cos\phi\cos\Omega\sin\psi-\sin\phi\cos\psi & -\sin\phi\cos\Omega\sin\psi+\cos\phi\cos\psi & \sin\Omega\sin\psi \\ \cos\phi\sin\Omega & \sin\phi\sin\Omega & \cos\Omega \end{bmatrix}. \tag{1}$$

The orientation of the $(hk\ell)$ reciprocal lattice vectors, $H_{hk\ell}$ is specified by the angles $\Theta_{hk\ell}$ and $\Phi_{hk\ell}$ in the 0-$a^*b^*c^*$ system and by the angles $\chi_{hk\ell}$ and $\eta_{hk\ell}$ in the 0-xyz system (Fig. 2). A unit vector along $H_{hk\ell}$ with angles $(\Theta_{hk\ell},\Phi_{hk\ell})$ can be transformed to the 0-xyz system with angles $(\chi_{hk\ell},\eta_{hk\ell})$ by using

$$\begin{bmatrix} \sin\chi_{hk\ell}\cos\eta_{hk\ell} \\ \sin\chi_{hk\ell}\sin\eta_{hk\ell} \\ \cos\chi_{hk\ell} \end{bmatrix} = T'(\phi,\Omega,\psi)\begin{bmatrix} \sin\Theta_{hk\ell}\cos\Phi_{hk\ell} \\ \sin\Theta_{hk\ell}\sin\Phi_{hk\ell} \\ \cos\Theta_{hk\ell} \end{bmatrix}, \tag{2}$$

where $T'(\phi,\Omega,\psi)$ is the transpose of the matrix $T(\phi,\Omega,\psi)$. If the sample possesses a fiber texture, the orientation function is independent of the Euler angle ϕ and the plane normal distribution functions are independent of the azimuthal angle $\eta_{hk\ell}$. The angles $\Theta_{hk\ell}$ and $\Phi_{hk\ell}$ are fixed by the crystallite system. In the case of a cubic system, where the a^*,b^* axes are taken to be the reciprocal a,b axes, these angles are given by

$$\cos\Theta_{hk\ell}=\frac{l}{(h^2+k^2+l^2)^{1/2}},$$
$$\cos\Phi_{hk\ell}=\frac{h}{(h^2+k^2)^{1/2}}. \tag{3}$$

THEORY

The basic equations relating the orientation function to the measured pole density functions were given by Roe.[1] It is assumed that the film has a fiber texture or one is artificially generated by an external rotation about the normal. Under these conditions, $w(\Omega,\psi)$, the orientation function is defined such that $w(\Omega,\psi)\sin\Omega d\Omega d\psi$ is the probability of finding a crystallite oriented in the angular range between (Ω,ψ) and $(\Omega+d\Omega,\psi+d\psi)$. We require that

$$\int_0^{2\pi}\int_0^{\pi} w(\Omega,\psi)\sin\Omega d\Omega d\psi = 1. \tag{4}$$

The orientation function is expanded into a series of spherical harmonics as follows[1]

$$w(\Omega,\psi)=\sum_{n=0}^{\infty} A_{n0}\,P_n^0(\cos\Omega) + 2\sum_{n=1}^{\infty}\sum_{m=1}^{n}\left[A_{nm}\,P_n^m(\cos\Omega)\cos m\psi + B_{nm}\,P_n^m(\cos\Omega)\sin m\psi\right], \tag{5}$$

where $P_n^m(\cos\Omega)$ is the normalized associated Legendre polynomial. The plane normal distribution functions relative to the random orientation $g_{hk\ell}(\chi)$ is defined as

$$g_{hk\ell}(\chi)=\frac{I_{hk\ell}(\chi)}{\int_0^{\pi} I_{hk\ell}(\chi)\sin\chi d\chi}, \tag{6}$$

where $I_{hk\ell}(\chi)$ is the diffracted intensity from planes with indices $(hk\ell)$, measured at an angle χ to the fiber axis. The function $g_{hk\ell}(\chi)$ can be expanded in a series of normalized Legendre polynomials,[1]

$$g_{hk\ell}(\chi)=\sum_{n=0}^{\infty} G_n^{hk\ell}P_n(\cos\chi), \tag{7}$$

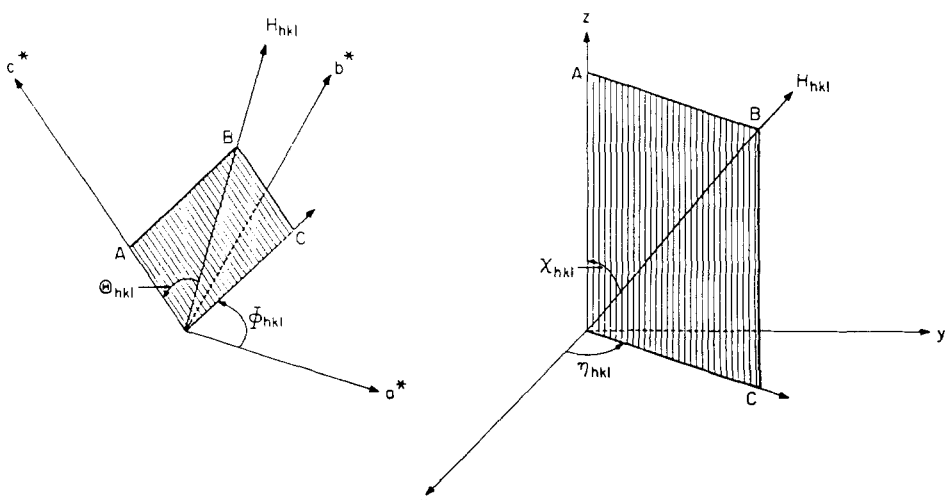

FIG. 2. Interrelationship of angle pairs $[\Theta_{hk\ell}$ (not the Bragg angle), $\Phi_{hk\ell}]$, and $[\chi_{hk\ell},\eta_{hk\ell}]$ to $H_{hk\ell}$ with a^*,b^*,c^* (left side), and specimen axes x,y,z (right side).

where the coefficient $G_n^{hk\ell}$ can be determined from

$$G_n^{hk\ell} = \int_0^{\pi} g_{hk\ell}(\chi) P_n(\cos\chi)\sin\chi d\chi. \tag{8}$$

In the case of random orientation [$g_{hk\ell}(\chi)$ is independent of χ] only $G_0^{hk\ell} \neq 0$. Since the plane normal distribution function on one half of the sphere is the same as the other half.

$$G_n^{hk\ell} = 0, \tag{9}$$

for n odd. Roe[1] has shown that

$$\begin{aligned} G_n^{hk\ell} &= 2\pi\left(\frac{2}{2n+1}\right)^{1/2}\Big\{A_{n0}\, P_n^0(\cos\Theta_{hk\ell}) + 2\sum_{m=1}^{n}(-1)^m \\ &\times [A_{mn}\, P_n^m(\cos\Theta_{hk\ell}) \\ &\cos m\Phi_{hk\ell} + B_{nm}\, P_n^m(\cos\Theta_{hk\ell})\sin m\Phi_{hk\ell}]\Big\}. \end{aligned} \tag{10}$$

For a random powder all the coefficients of the orientation function vanish but for $A_{0,0}$. Moreover, since $P_0^0(\cos\Theta_{hk\ell})$ is independent of $\cos\Theta_{hk\ell}$, $G_0^{hk\ell}$ is independent of the indices $(hk\ell)$ and is equal to $2\pi\sqrt{2}A_{0,0}\, P_0^0$. The normalized value for $G_0^{hk\ell}$ and $A_{0,0}$ are equal to $1/\sqrt{2}$ and $1/(2\pi\sqrt{2})$, respectively. In the case of oriented samples, even though the other coefficients do not vanish, the value for $G_0^{hk\ell}$ and $A_{0,0}$ remain the same. The coefficients $G_n^{hk\ell}$ of the plane normal distributions are related to the coefficients A_{nm}'s and B_{nm}'s of the orientation function expansion through an nth order trignometric expression of angles $\Theta_{hk\ell}$ and $\Phi_{hk\ell}$, the polar and azimuthal angles of the reciprocal lattice vector $H_{hk\ell}$, in the coordinate system 0-$a^*b^*c^*$. The number of plane normal distributions required to determine the orientation function of the sample, to an order of n, can be seen to be equal to $(2n+1)$ from Eq. (10). This number can be decreased due to crystal symmetry. The following expansion was found to be a useful form for obtaining the normalized associated Legendre polynomials $P_n^m(\xi)$[4]

$$P_n^m(\xi) = (\xi^2 - 1)^{m/2}\sum_{p=0}^{n-m} J(n,m,p)\xi^p \quad (n,m,p \text{ even}), \tag{11}$$

with

$$J(n,m,p) = \left[\frac{2n+1}{2}\frac{(n-m)!}{(n+m)!}\right]^{1/2} \times (-1)^{(n-p)/2}\frac{(n+m+p-1)!!}{p!(n-m-p)!!}, \tag{12}$$

where the notation

$$(N)!! = N(N-2)(N-4)...$$

is used. Legendre polynomials are generated from the recurrence formula

$$P_{n+1}(\cos\chi) = \frac{2n+1}{n+1}\cos\chi\, P_n(\cos\chi) - \frac{n}{n+1}P_{n-1}(\cos\chi), \tag{13}$$

where $P_0(\cos\chi) = 1$ and $P_1(\cos\chi) = \cos\chi$. After evaluating the Legendre polynomials using Eq. (13) (for a particular value of $\cos\chi$), they are normalized by multiplying by a factor of $(2/(2n+1))^{1/2}$.

CUBIC SYMMETRY

Since the crystallite coordinate system has been chosen to be the reciprocal a^*, b^*, c^* axes, cubic symmetry can be discussed in terms of equivalent reciprocal lattice vectors. The equivalence of $H_{hk\ell}$ reciprocal lattice vectors is due to the presence of three mirror planes of symmetry, parallel and perpendicular to the c^* axis plus a fourfold rotation symmetry around the c^* axis, in a cubic crystal. From Eqs. (3) and (10) and the symmetry conditions, it can easily be deduced that all the coefficients, B_{nm} of the orientation function vanish. Also, $A_{nm} \neq 0$ only if m is an integral multiple of four. Roe[5] has shown that the equivalence of reciprocal lattice vectors requires that not all nonvanishing coefficients A_{nm}, for a particular order of n, are independent. In fact, the maximum number of independent coefficients for any order n, till $n = n_{\max}$, can be written as

$$\nu_n(\max) = \mathrm{Int}(n_{\max}/12) + 1, \tag{14}$$

where $\mathrm{Int}(n_{\max}/12)$ is the integer part of the value $n_{\max}/12$. The number of nonvanishing coefficients A_{nm} for a particular order n, is given by

$$\mu_n = \mathrm{Int}(n/4) + 1. \tag{15}$$

If $H_{hk\ell}$ and $H_{\ell kh}$ are to be equivalent, we require that the following matrix equation be satisfied[5]

$$\begin{bmatrix} Z'_{n00} - \left(\frac{2n+1}{2}\right)^{1/2} & , & 2Z'_{n40}, & , & 2Z'_{nN0} \\ Z'_{n04} & , & 2Z'_{n44} - \left(\frac{2n+1}{2}\right)^{1/2}, & , & 2Z'_{nN4} \\ \cdot & & \cdot & & \cdot \\ \cdot & & \cdot & & \cdot \\ \cdot & & \cdot & & \cdot \\ \cdot & & \cdot & & \cdot \\ Z'_{n0N} & , & 2Z'_{n4N}, & , & 2Z'_{nNN} - \left(\frac{2n+1}{2}\right)^{1/2} \end{bmatrix} \begin{bmatrix} A_{n0} \\ A_{n4} \\ \\ A_{nN} \end{bmatrix} = 0. \tag{16}$$

TABLE I. Symmetry requirements of A_{nm} for cubic crystals, from $n = 24$ to $n = 46$.

Linearly dependent coefficients	Linearly dependent coefficients
$A_{24,0} = 0.2394533A_{24,16}+0.7506842A_{24,20}+1.3527187A_{24,24}$	$A_{36,16}=0.4630997A_{36,24}-0.5922425A_{36,28}+0.8232896A_{36,32}+0.03241365A_{36,36}$
$A_{24,4}= -0.2659120A_{24,16}-0.5622099A_{24,20}+0.9766433A_{24,24}$	$A_{36,20} = -0.7331106A_{36,24}+1.1782936A_{36,28}+0.3182074A_{36,32}+0.003894250A_{36,36}$
$A_{24,8} = 0.3622187A_{24,16}-0.103403A_{24,20}+0.3563462A_{24,24}$	$A_{38,0} = -0.4516079A_{38,28}-0.67605321A_{38,32}-0.8597611A_{38,36}$
$A_{24,12} = -0.5887667A_{24,16}+1.2249962A_{24,20}+0.06552806A_{24,24}$	$A_{38,4} = 0.4552974A_{38,28}+0.4760332A_{38,32}-0.1104550A_{38,36}$
$A_{26,0} = -0.6345848A_{26,20}-0.9440440A_{26,24}$	$A_{38,8} = -0.4589022A_{38,28}+0.06741741A_{38,32}+0.8819213A_{38,36}$
$A_{26,4} = 0.6194214A_{26,20}+0.1579850A_{26,24}$	$A_{38,12} = 0.4319049A_{38,28}-0.6772946A_{38,32}+0.8447258A_{38,36}$
$A_{26,8} = -0.5249468A_{26,20}+1.0935636A_{26,24}$	$A_{38,16} = -0.2942929A_{38,28}+0.6127140A_{38,32}+0.3484093A_{38,36}$
$A_{26,12} = 0.1526602A_{26,20}+0.5694759A_{26,24}$	$A_{38,20} = -0.1021267A_{38,28}+0.8073734A_{38,32}+0.07355567A_{38,36}$
$A_{26,16} = 0.7892093A_{26,20}+0.09553932A_{26,24}$	$A_{38,24} = 0.6708204A_{38,28}+0.2301144A_{38,32}+0.007685357A_{38,36}$
$A_{28,0} = 0.3740640A_{28,20}+0.7810819A_{28,24}+1.3029906A_{28,28}$	$A_{40,0} = 0.2687324A_{40,28}+0.5848670A_{40,32}+0.7375370A_{40,36}+1.1928232A_{40,40}$
$A_{28,4} = -0.3917853A_{28,20}-0.4966444A_{28,24}+0.9835918A_{28,28}$	$A_{40,4} = -0.2789661A_{40,28}-0.5069377A_{40,32}-0.2373559A_{40,36}+0.9787244A_{40,40}$
$A_{28,8} = 0.4410513A_{28,20}-0.3027326A_{28,24}+0.4174167A_{28,28}$	$A_{40,8} = 0.3103257A_{40,28}+0.2588738A_{40,32}-0.6550715A_{40,36}+0.5384887A_{40,40}$
$A_{28,12} = -0.4847254A_{28,20}+1.0397492A_{28,24}+0.09642897A_{28,28}$	$A_{40,12} = -0.3624310A_{40,28}+0.1757258A_{40,32}+0.5140270A_{40,36}+0.1962690A_{40,40}$
$A_{28,16} = 0.3026250A_{28,20}+0.5271712A_{28,24}+0.01096018A_{28,28}$	$A_{40,16} = 0.4216925A_{40,28}-0.6899967A_{40,32}+0.8934426A_{40,36}+0.04632647A_{40,40}$
$A_{30,0} = -0.2012063A_{30,20}-0.6225923A_{30,24}-0.9093188A_{30,28}$	$A_{40,20} = -0.4169401A_{40,28}+0.7302004A_{40,32}+0.4163062A_{40,36}+0.006851606A_{40,40}$
$A_{30,4} = 0.2181183A_{30,20}+0.5395815A_{30,24}+0.4235354A_{30,28}$	$A_{40,24} = 0.9454766A_{40,28}+0.6885383A_{40,32}+0.8295230A_{40,36}+0.0005942216A_{40,40}$
$A_{30,8} = -0.2769528A_{30,20}-0.2389022A_{30,24}+1.0377361A_{30,28}$	$A_{42,0} = -0.1492172A_{42,28}-0.4675634A_{42,32}-0.6581057A_{42,36}-0.8380780A_{42,40}$
$A_{30,12} = 0.4062592A_{30,20}-0.4020019A_{30,24}+0.6874909A_{30,28}$	$A_{42,4} = 0.1576499A_{42,28}+0.4467373A_{42,32}+0.4037325A_{42,36}-0.1655360A_{42,40}$
$A_{30,16} = -0.6592803A_{30,20}+1.2130033A_{30,24}+0.1892425A_{30,28}$	$A_{42,8} = -0.1856424A_{42,28}- 0.3702801A_{42,32}+0.2193959A_{42,36}+0.8051003A_{42,40}$
$A_{32,0} = 0.5297804A_{32,24}+0.7766137A_{32,28}+1.2607394A_{32,32}$	$A_{42,12} = 0.2423910A_{42,28}+0.1928967A_{42,32}-0.7334047A_{42,36}+0.8812757A_{42,40}$
$A_{32,4} = -0.5288543A_{32,24}-0.4074700A_{32,28}+0.9851110A_{32,32}$	$A_{42,16} = -0.3408087A_{42,28}+0.1608563A_{42,32}+0.3696329A_{4}+0.4285367A_{42,40}$
$A_{32,8} = 0.5080249A_{32,24}-0.4657722A_{32,28}+0.4662348A_{32,32}$	$A_{42,20} = 0.5296222A_{42,28}-0.7251012A_{42,32}+0.8427769A_{43,36}+0.1123580A_{42,40}$
$A_{32,12} = -0.3932762A_{32,24}+0.8721006A_{32,28}+0.1304745A_{32,32}$	$A_{42,24} = -0.808773A_{42,28}+1.1314072A_{42,32}+0.4438826A_{42,36}+0.01768675A_{42,40}$
$A_{32,16} = 0.006020042A_{32,24}+0.7264686A_{32,28}+0.02058378A_{32,32}$	
$A_{32,20} = 0.7342231A_{32,24}+0.1631825A_{32,28}+0.001642166A_{32,32}$	
$A_{34,0} = -0.3898767A_{34,24}-0.6664749A_{34,28}-0.8837449A_{34,32}$	
$A_{34,4} = 0.3275050A_{34,24}+0.5246072A_{34,28}-0.4225494A_{34,32}$	
$A_{34,8} = -0.3672791A_{34,24}-0.08929320A_{34,28}+0.9604242A_{34,32}$	
$A_{34,12} = 0.4257659A_{34,24}-0.5699147A_{34,28}+0.7834093A_{34,32}$	
$A_{34,16} = -0.4491263A_{34,24}+0.8884650A_{34,28}+0.2644064A_{34,32}$	
$A_{34,20} = 0.1942924A_{34,24}+0.6210609A_{34,28}+0.04086180A_{34,32}$	
$A_{36,0} = 0.1721675A_{36,24}+0.5344552A_{36,28}+0.7523050A_{36,32}+1.2244126A_{36,36}$	
$A_{36,4} = -0.1838136A_{36,24}-0.4934991A_{36,28}-0.3112313A_{36,32}+0.9838817A_{36,36}$	
$A_{36,8} = 0.2232129A_{36,24}+0.3455721A_{36,28}-0.5894719A_{36,32}+0.5058974A_{36,36}$	
$A_{36,12} = -0.3058257A_{36,24}-0.01113577A_{36,28}+0.7046844A_{36,32}+0.1641933A_{36,36}$	

TABLE I. (Cont'd).

Linearly dependent coefficients	Linearly dependent coefficients
$A_{44,0} = 0.3904564A_{44,32}+0.6043369A_{44,36}+0.7211224A_{44,40}$ $+1.1649890A_{44,44}$	$A_{46,0} = -0.2328325A_{46,32}-0.5218439A_{46,36}-0.6508036A_{46,40}$ $-0.8190778A_{46,44}$
$A_{44,4} = -0.3954859A_{44,32}-0.4863782A_{44,36}-0.1715037A_{44,40}$ $+0.9730059A_{44,44}$	$A_{46,4} = 0.2408480A_{46,32}+0.4763726A_{46,36}+0.3486478A_{46,40}$ $-0.20990315A_{46,44}$
$A_{44,8} = 0.4072948A_{44,32}+0.14441401A_{44,36}-0.6928258A_{44,40}$ $+0.5653261A_{44,44}$	$A_{46,8} = -0.2656777A_{46,32}-0.3289858A_{46,36}+0.3236421A_{46,40}$ $+0.7312906A_{46,44}$
$A_{44,12} = -0.4124342A_{44,32}+0.3447960A_{44,36}+0.3400350A_{44,40}$ $+0.2263988A_{44,44}$	$A_{46,12} = 0.3088232A_{46,32}+0.05415386A_{46,36}-0.7063938A_{46,40}$ $+0.9000794A_{46,44}$
$A_{44,16} = 0.3746047A_{44,32}-0.7106222A_{44,36}+0.9033880A_{44,40}$ $+0.06147884A_{44,44}$	$A_{46,16} = -0.3681822A_{46,32}+0.3497156A_{46,36}+0.1071152A_{46,40}$ $+0.4998413A_{46,44}$
$A_{44,20} = -0.2125752A_{44,32}+0.3761753A_{44,36}+0.5274659A_{44,40}$ $+0.01103715A_{44,44}$	$A_{46,20} = 0.4225179A_{46,32}-0.7365662A_{46,36}+0.8619584A_{46,40}$ $+0.1576050A_{46,44}$
$A_{44,24} = -0.1860984A_{44,32}+0.8390027A_{44,36}+0.1423797A_{44,40}$ $+0.001261225A_{44,44}$	$A_{46,24} = -0.3840694A_{46,32}+0.5767281A_{46,36}+0.5393598A_{46,40}$ $+0.02960701A_{46,44}$
$A_{44,28} = 0.6026242A_{44,32}+0.2938476A_{44,36}+0.01862208A_{44,40}$ $+0.00008453298A_{44,44}$	$A_{46,28} = 0.7368389A_{46,36}+0.1339869A_{46,40}+0.003236213A_{46,44}$

where N is the maximum multiple of four less than n,Z'_{n00} stands for $Z_{n00}(0°)$ etc., and $Z_{nmp}(0°)$, known as the Jacobi polynomial of order n,m, p and angle zero degrees, is given by[5]

$$Z_{nmp}(0°) = \left(\frac{2n+1}{2}\right)^{1/2} 2^{-n}[(n+m)!(n-m)!(n+p)!(n-p)!]^{1/2} \times \sum_{j=0}^{\infty} (-1)^j[(n-m-j)!(n+p-j)!(m-p+j)!j!]^{-1}. \quad (17)$$

Any other equivalent reciprocal lattice vector in the cubic system can be generated through a combination of symmetry transformations involving all equivalent vectors $H_{hk\ell}$ within a set of multiplicity j. Hence, no other symmetry conditions need be satisfied. From Eqs. (10) and (14), one can see that the orientation function can be expanded to the 46th order, by having experimental data for just four plane normal distributions. But, additional data are required for an actual data set due to series truncation error, extrapolation error, and statistical error in the data. Roe[5] has given the interdependency among the coefficients of a particular order of n to $n = 22$. Here the relationships are extended from $n = 24$ to $n = 46$. Table I lists the extended relationships from $n = 24$ to $n = 46$ calculated in triple precision arithmetic.

To illustrate these properties, consider the reciprocal lattice vector $H_{hk\ell}$ and an orientation function, truncated at $n = 4$. $G_0^{hk\ell}$ has already been shown to be a constant. From Table I of Ref. 5 and Eq. (10), $G_2^{hk\ell}$ and $G_4^{hk\ell}$ are given by

$$G_2^{hk\ell} = 0$$

$$G_4^{hk\ell} = 2\pi(2/9)^{1/2}[A_{4,0}(P_4^0(\cos\Theta_{hk\ell}) + 1.1952286\,P_4^4(\cos\Theta_{hk\ell})\cos 4\Phi_{hk\ell}]. \quad (18)$$

Expanding $P_4^0(\cos\Theta_{hk\ell})$ and $P_4^4(\cos\Theta_{hk\ell})$ in powers of

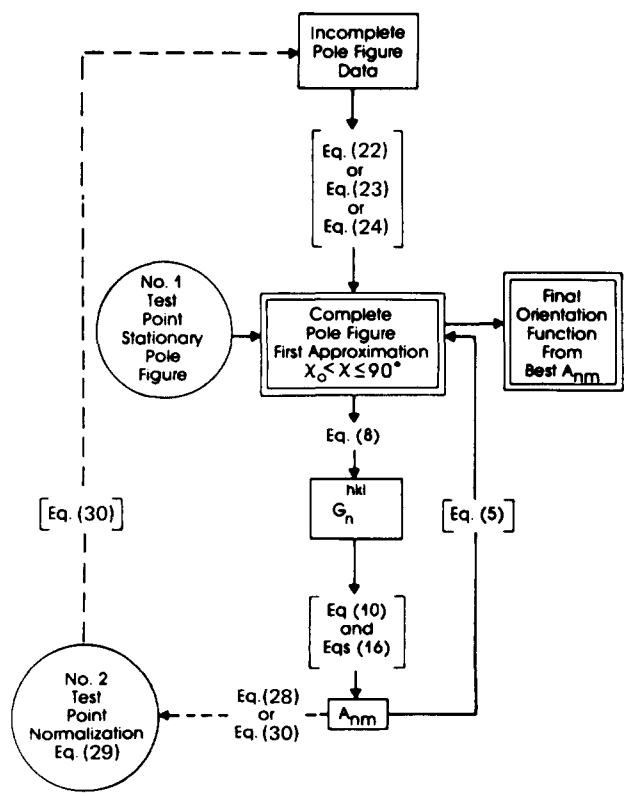

FIG. 3. Flow diagram for computer program providing orientation function and film thickness.

cos $\Theta_{hk\ell}$, and cos $4\Phi_{hk\ell}$ in terms of cos $\Phi_{hk\ell}$ (see Refs. 6 and 7), one finds

$$G_4^{hk\ell} = 2\pi A_{4,0}\,[0.375 - 3.75\cos^2\Theta_{hk\ell} + 4.375\cos^4\Theta_{hk\ell} + 0.625\sin^4\Theta_{hk\ell}(8\cos^4\Phi_{hk\ell} - 8\cos^2\Phi_{hk\ell} + 1)]. \quad (19)$$

Substituting Eq. (3) in Eq. (19) and simplifying,

$$G_4^{hk\ell} = 2\pi A_{4,0}\left(0.375 + \frac{0.625(h^4 + k^4 + \ell^4)}{(h^2 + k^2 + \ell^2)^2}\right)\left(- \frac{3.75(h^2k^2 + \ell^2h^2 + k^2\ell^2)}{(h^2 + k^2 + \ell^2)^2}\right). \quad (20)$$

From Eq. (20) it is seen that $G_4^{hk\ell}$ is identical for all equivalent reciprocal lattice vectors in the cubic system. Similarly, with more algebraic computation, it can be shown that $G_n^{hk\ell}$ is the same for all equivalent reciprocal lattice vectors, for any n up to $n = 46$. Consequently, the plane normal distribution function $g_{hk\ell}(\chi)$ is identical for all equivalent reciprocal lattice vectors in the cubic system. This requirement is imposed when Eqs. (16) are satisfied.

INITIAL EXTRAPOLATION

To obtain the nth coefficient of the plane normal distribution function expansion, one must evaluate the integral given in Eq. (8). If data are available in the range $0 \leqslant \chi_{hk\ell} \leqslant \chi_0$, a suitable initial extrapolation has to be made for the plane normal distributions from $\chi_{hk\ell} = \chi_0$ to $\chi_{hk\ell} = 90°$, so as to evaluate the definite integral given in Eq. (8). Two types of simple approximations are considered, i.e., the zero- and first-order approximations. Both make use of the condition

$$\int_0^{\pi} g_{hk\ell}(\chi)\sin\chi d\chi = 1. \quad (21)$$

In the case of the zero-order approximation, the extrapolation is approximated by a constant value, which is given by

$$g_{hk\ell}^{ex} = \frac{1 - 2\int_0^{\chi_0} g_{hk\ell}(\chi)\sin\chi d\chi}{2\cos\chi_0}, \quad g_{hk\ell}^{ex} > 0. \quad (22)$$

If the constant value calculated from Eq. (22) turns out to be less than zero, it is set equal to zero. In the case of the first-order approximation, an equation of the form $g^{(ex)} = m\cos\chi + c$ is used to fit the extrapolation region. This second approximation gives

$$g_{hk\ell}^{(ex)}(\chi) = -g_{hk\ell}(\chi_0) - \left(\frac{1 - 2\int_0^{\chi_0} g_{hk\ell}(\chi)\sin\chi d\chi}{\cos^2\chi_0} - \frac{2g_{hk\ell}(\chi_0)}{\cos\chi_0}\right) \times (\cos\chi - \cos\chi_0), \quad (23)$$

where $g_{hk\ell}^{ex} > 0$ for $\chi_0 \leqslant \chi \leqslant 90°$. When $g_{hk\ell}^{ex}(90°)$ as calculated by Eq. (23) attains a negative value, the approximation must be modified because a linear extrapolation between the point $g_{hk\ell}(\chi_0)$ and $g_{hk\ell}(90°) = 0$ contributes too much to the integral [Eq. (23)]. Alternatively, one must force the straight line to zero at $\chi' < 90°$. In this extrapolation, there are two linear portions for the range $\chi_0 \leqslant \chi \leqslant 90°$ interconnected at χ'. The nonzero portion extending to χ' is given by

$$g_{hk\ell}^{ex}(\chi) = -\frac{g_{hk\ell}(\chi_0)}{(\cos\chi_0 - \cos\chi')}(\cos\chi_0 - \cos\chi) + g_{hk\ell}(\chi_0), \quad (24)$$

where

$$\cos\chi' = \cos\chi_0 - \left(\frac{1 - 2\int_0^{\chi_0} g_{hk\ell}(\chi)\sin\chi d\chi}{g_{hk\ell}(\chi_0)}\right). \quad (25)$$

ITERATIVE PROCEDURES

Experimental data from $\chi = 0$ to $\chi = \chi_0$, along with the initial extrapolations are used to generate the first set of plane normal distribution coefficients, $G_n^{hk\ell}$ from Eq. (8) (see Fig. 3). These sets of coefficients are used to generate the orientation function using Eqs. (10) and a least-squares routine. Equations (10) are simplified for the particular case of cubic crystallites by means of Eqs. (16). The orientation function coefficients A_{nm} are used to determine a second approximation to the unmeasured region for all plane normal distribution curves. This iterative process is controlled at "No. 1 Test Point" and is continued until the extrapolations for all plane normal distribution curves become stationary. At this point, the extended plane normal distributions may be used to determine the orientation function in the polycrystalline film by using a procedure given in the next section.

TABLE II. Angle between (hkl) and (110) planes for crystallographic cubic symmetry.[11]

hkl	χ	cos χ
(200)	45.00°, 90.00°	0.71, 0.00
(211)	30.00°, 54.74°, 73.22°, 90.00°	0.87, 0.58, 0.29, 0.00
(220)	60.00°, 90.00°	0.50, 0.00
(301)	26.56°, 47.87°, 63.43°, 77.08°	0.89, 0.67, 0.45, 0.22
(222)	35.26°, 90.00°	0.82, 0.00
(321)	19.11°, 40.89°, 55.46°, 67.79°, 79.11°	0.94, 0.76, 0.57, 0.38, 0.19
(210)	18.43°, 50.77°, 71.56°	0.95, 0.63, 0.32
(221)	19.47°, 45.00°, 76.37°, 90.00°	0.94, 0.71, 0.24, 0.00
(311)	31.48°, 64.76°, 90.00°	0.85, 0.43, 0.00
(320)	11.31°, 53.96°, 66.91°, 78.69°	0.98, 0.59, 0.39, 0.20
(410)	30.96°, 46.69°, 59.04°, 80.13°	0.86, 0.69, 0.51, 0.17
(322)	30.96°, 46.69°, 80.13°, 90.00°	0.86, 0.69, 0.17, 0.00
(411)	33.56°, 60.00°, 70.53°, 90.00°	0.83, 0.50, 0.33, 0.00

DETERMINATION OF THICKNESS

The values of $g_{hk\ell}(\chi)$ are calculated using Eq. (6). Equation (6) can be modified as

$$g_{hk\ell}(\chi) = \frac{I_{hk\ell}(\chi)}{2I^{P}_{hk\ell}}, \tag{26}$$

where $I^{P}_{hk\ell}$ is the integrated intensity for the powder sample of the same material as the thin film under identical diffraction conditions. Powder and thick film intensities are related by the integral

$$I^{P}_{hk\ell} = \frac{\int_0^{\pi} I_{hk\ell}(\chi)\sin\chi d\chi}{\int_0^{\pi}\sin\chi d\chi}. \tag{27}$$

Equation (26) is valid for a thick sample. The intensity from a film, $I^{f}_{hk\ell}(\chi)$, can be used provided one divides by the absorption term which makes the film to appear infinite in thickness,[8] i.e.,

$$g_{hk\ell}(\chi) = \frac{I^{f}_{hk\ell}(\chi)}{2I^{P}_{hk\ell}}\left(1 - e\frac{-2\mu t}{\sin\theta_{hk\ell}\cos\chi}\right)^{-1} \tag{28}$$

where μ is the linear absorption coefficient of the thin film, $\theta_{hk\ell}$ is the Bragg angle for planes with indices $hk\ell$, and t is the thickness of the film. The thickness of the film is determined by including the film thickness in the iterative process, and finding the thickness at which the integral

$$\int_0^{\pi} g_{hk\ell}(\chi)\sin\chi d\chi$$

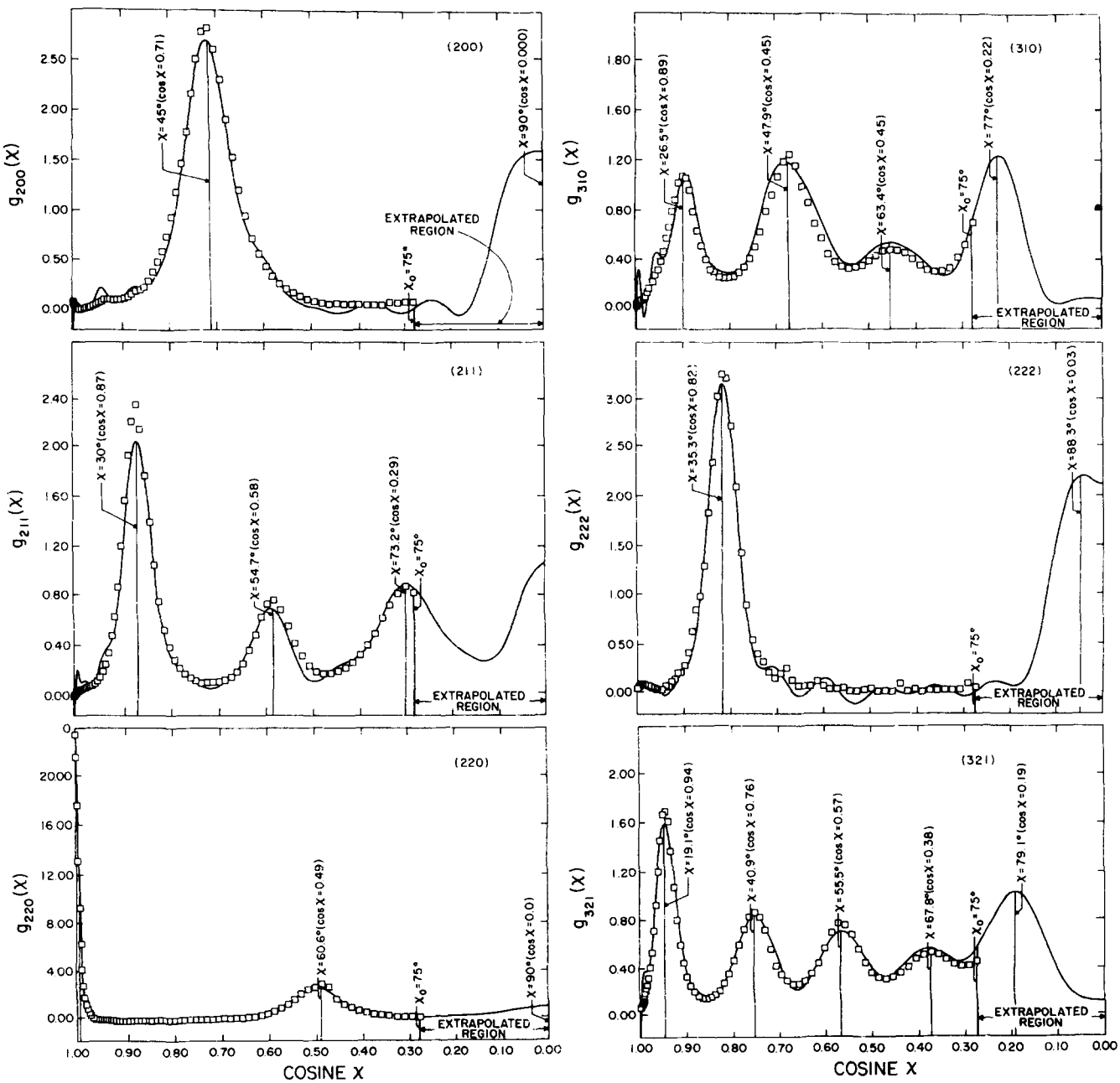

FIG. 4. Plane normal distributions for (200), (211), (220), (310), (222), and (321) planes. Experimental points and continuous curves generated from Eq. (5) are illustrated. The experimental cutoff is at $\chi = 75°$.

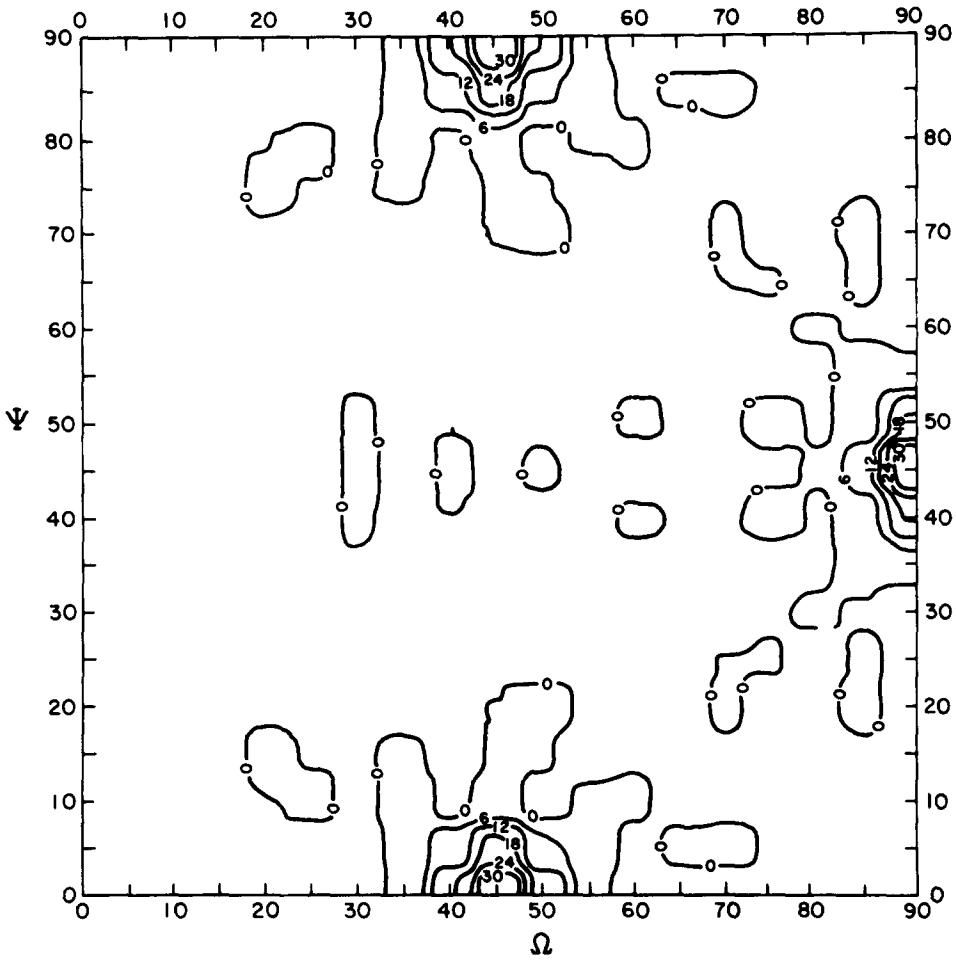

FIG. 5. Orientation function map for a sputter deposited Mo film on (111) Si.

averaged over all stationary plane normal distributions is within 7% of unity. The criterion adopted for this can be written as

$$0.93 < \left[\int_0^{\pi} g_{hk\ell}(\chi) \sin \chi \, d\chi \right]_{hk\ell} \leq 1.07 \tag{29}$$

is established at test point No. 2. By means of Eqs. (28) and (29), one can see that if the average of the integral in Eq. (29) for all $hk\ell$ is less than 0.93, the thickness estimate should be decreased and if it is greater than 1.07, it should be increased.

A general equation for $g_{hk\ell}(\chi)$ can be written as

$$g_{hk\ell}(\chi) = \frac{I_{hk\ell}(\chi)}{2I^{P}_{hk\ell}} \left(1 - e - \frac{-2\mu t}{\sin \theta_{hk\ell} \cos \chi} \right)^{-1} A_m(\theta_{hk\ell}, \chi), \tag{30}$$

where $A_m(\theta_{hk\ell}, \chi)$ is a parameter used for correcting the intensity loss due to static displacements in the film as compared to the ideal powder sample. This was assumed to be equal to one in the present analysis. When a film contains oversize or undersize atoms in either substitutional or interstitial positions, the resultant static displacements produce a systematic decrease in the integrated intensities of the Bragg reflections.[9,10] In order to determine $A_m(\theta_{hk\ell}, \chi)$, the thickness t must be obtained by some independent measurement such as weight gain or by interference microscopy. The normalization requirement as given by Eq. (29) allows $A_m(\theta_{hk\ell}, \chi)$ to be determined relative to a powder standard which is unaffected by static displacements.

RESULTS AND DISCUSSION

The Mo thin film sputtered onto a (111) Si single crystal substrate contained a fiber texture with the (110) planes preferentially oriented parallel to the substrate. If one assumes that the thin film is a pseudo single crystal with 110 planes aligned parallel to the 111 planes of the Si single crystal substrate, one can interrelate the peak positions for the (200), (211), (220), (310), (222), and (321) planes. These angles are given in Table II. Noting the plane normal distributions of all six plane normals from 0–75° (Fig. 4) and the interplanar angles, one can clearly see that below 75°, all the plane normal distributions have peaked at angles as predicted by Table II. Hence, one expects all the extrapolations obtained by the iterative process to peak at angles (above 75°) as given in Table II. From Fig. 4, it is evident that this is clearly the case. The extrapolations shown in Fig. 4 used data up to 75° for all six plane normal distributions and seven iterations. A two-dimensional map of the orientation function as a function of the Euler angles Ω and ψ is given in Fig. 5. This figure shows that the orientation function is sharply peaked at Euler an-

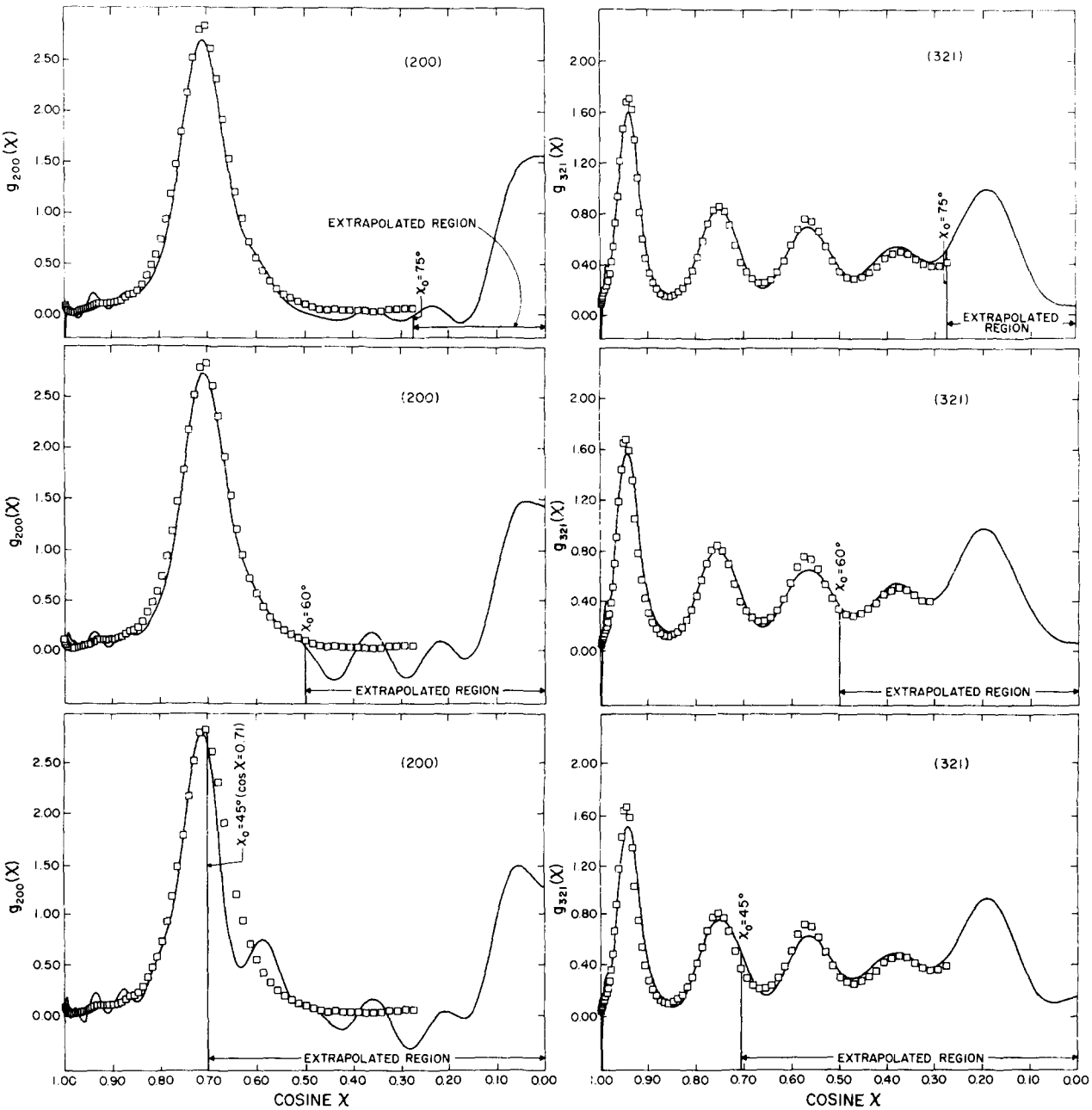

FIG. 6. Illustration of errors generated by truncations at $\chi_0 = 60°$ and 45° for the (200) and (321) planes.

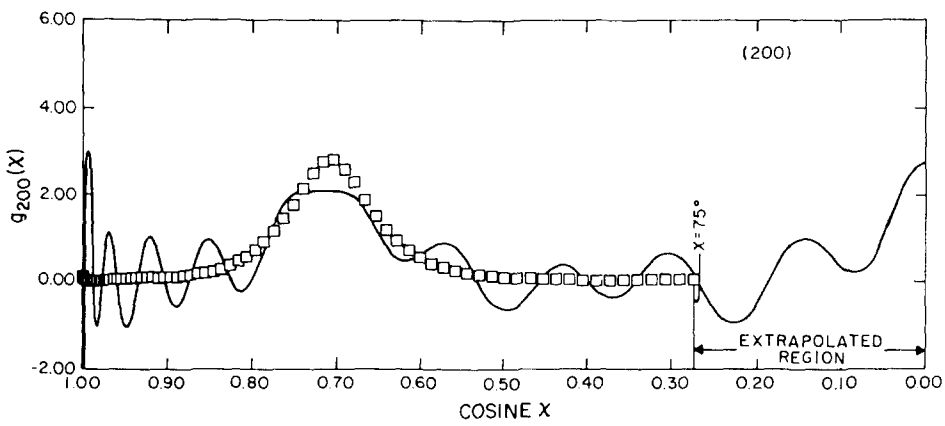

FIG. 7. Example of largest errors (200 plane normal distribution) after truncating from 6 to 5 plane normal distributions.

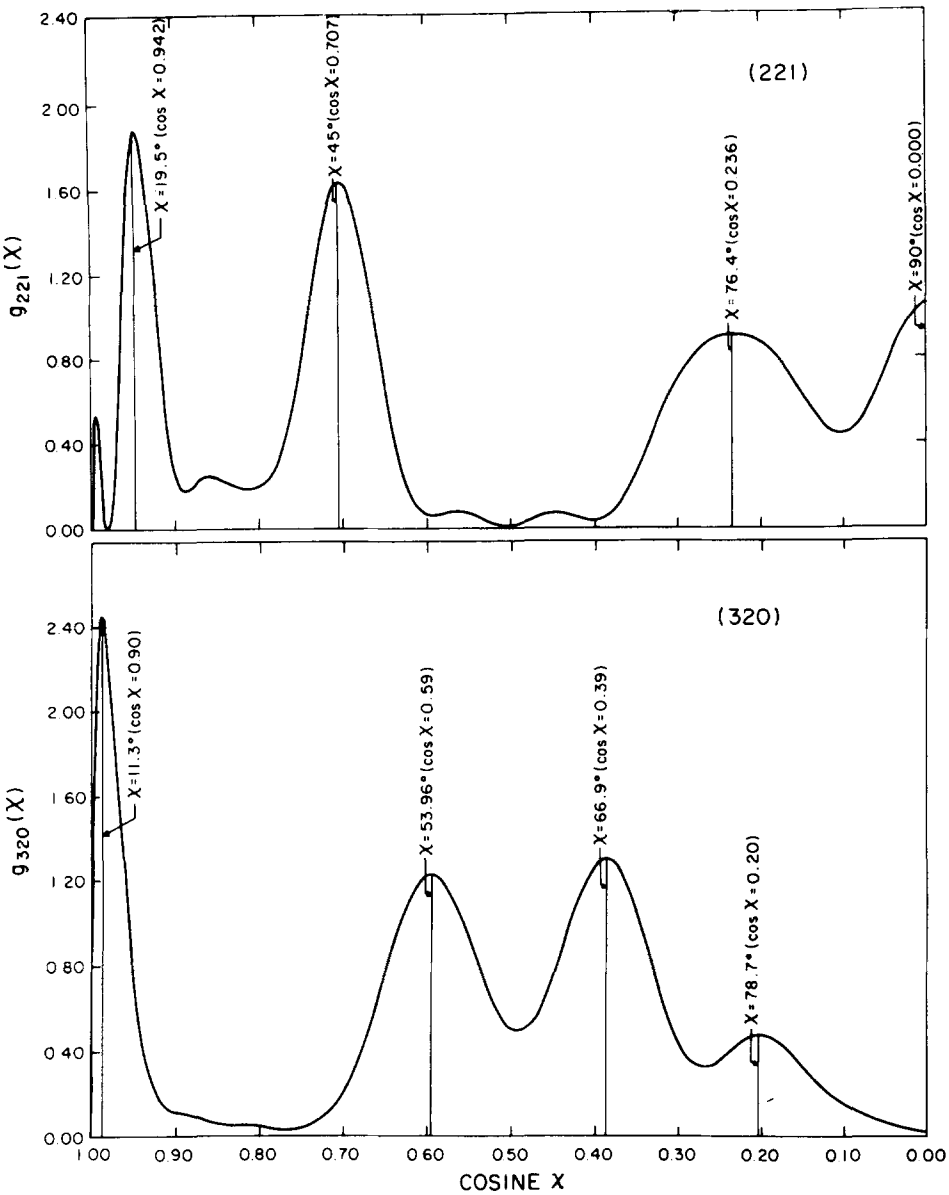

FIG. 8. Generated (221), (320) plane normal distributions not measureable by x-ray diffraction.

gles of $(\Omega,\psi) = (45°,0°)$, $(45°,90°)$, and $(90°,45°)$ and is symmetric about the $\psi = 45°$ axis, due to the cubic symmetry of the crystallites. The final orientation function obtained by using the zero-order approximation as the initial guess is almost identical with the orientation function obtained by using the first order approximation as the initial guess. Both are based upon seven iterations.

The same analysis was carried out using data truncated at 60° and 45°, for all plane normal distributions. The plane normal distributions terminated at 45°, 60° follow the experimental data with some oscillations. Also, the extrapolations obtained above 75° were essentially the same for all three cases. The extrapolation obtained for the reciprocal lattice vectors (200) and (321) truncated at 60° and 45° are given in Fig. 6. But, the orientation function derived using five plane normal distribution data up to $\chi = 75°$, generated the sixth plane normal distributions with a significant amount of spurious oscillations. The (200), however, represents the worst case (Fig. 7). The above results as well as others indicate that additional $hk\ell$ data might be more significant than additional χ data. The orientation function obtained using six plane normal distribution data to an angle of $\chi = 75°$, was used to generate seven unmeasured plane normal distributions (311, 210, 221, 320, 410, 322, and 411). All the distributions peak at angles predicted from Table II. Examples of the (221) and (320) plane normal distributions are given in Fig. 8. The thickness estimate of the film from this analysis was 1.21 μ which compares favorably with suppliers value of 1.14 μ.

ACKNOWLEDGMENTS

Funding was made available by National Science Foundation Grant No. DMR-8000933. The authors would like to thank Mr. R. Yesensky for making his data available for this study.

[1]R. J. Roe and W. R. Krigbaum, J. Chem. Phys. **40**, 2608 (1964).
[2]P. R. Morris, Adv. X-Ray Anal. **18**, 514 (1975).
[3]C. R. Houska and V. Rao, Metall. Trans. **9A**, 1483 (1978).
[4]W. R. Krigbaum and R. J. Roe, J. Chem. Phys. **41**, 737 (1964).

[5]R. J. Roe, J. Appl. Phys. **37**, 2069 (1966).
[6]T. M. MacRobert, *Spherical Harmonics*, 3rd ed., (Pergamon, Oxford, 1967), pp. 113–133.
[7]*Handbook of Mathematical Functions*, 1st ed. (Dover, New York, 1965), pp. 65–93.
[8]R. Yesensky, V. Rao, and C. R. Houska, Thin Solid Films **79**, 27 (1981).
[9]D. T. Keating, J. Phys. Chem. Solids **29**, 771 (1968).
[10]T. Adler and C. R. Houska, J. Appl. Phys. **50**, 3288 (1979).
[11]*International Tables for X-Ray Crystallography* (Kynoch, Birmingham, 1959), Vol. II, pp. 120–122.